Neuron
Article

Frequency-Band Coupling in Surface EEG Reflects Spiking Activity in Monkey Visual Cortex

Kevin Whittingstall[1,*] and Nikos K. Logothetis[1,2]
[1]Max Planck Institute for Biological Cybernetics, Spemannstrasse 38, D-72076 Tübingen, Germany
[2]Division of Imaging Science and Biomedical Engineering, University of Manchester, Manchester M13 9PT, UK
*Correspondence: kevin.whittingstall@tuebingen.mpg.de
DOI 10.1016/j.neuron.2009.08.016

SUMMARY

Although the electroencephalogram (EEG) is widely used in research and clinical settings, its link to the underlying neural activity during sensory processing remains poorly understood. To investigate this, we made simultaneous recordings of surface EEG, intracortical local field potential, and multiunit activity (MUA) in the alert monkey visual cortex during presentation of natural movies. Using a general linear model, we show that in single trials, EEG power in the gamma band (30–100 Hz) and phase in delta band (2–4 Hz) are significant predictors of the MUA response. Specifically, we found that the MUA response was strongest only when increases in EEG gamma power occurred during the negative-going phase of the delta wave, thus revealing a frequency-band coupling mechanism that can be exploited to infer population spiking activity. This finding may open up a new dimension in the use and interpretation of EEG in normal and pathological conditions.

INTRODUCTION

The first electroencephalogram (EEG) recording was made over 80 years ago, and since then has become one of the most widely used tools for studying brain activity in humans (Lopes da Silva and Van Rotterdam, 1987). Its noninvasive nature makes it an ideal neuroimaging method that is routinely used in clinical applications as well as in neurophysiological research even after the advent of other noninvasive neuroimaging techniques, such as functional magnetic resonance imaging. Nevertheless, despite advancements in EEG technology that allow for the recording and localization of neural activity with ever increasing spatial resolution, it remains unknown which cortical processes are represented in the EEG signal and which are not. In particular, its relationship to the underlying spiking activity of a neuronal population is far from clear, especially when the neural processes under investigation reflect cognitive behavior.

For years, the dominant view has been that the surface EEG signal reflects synchronized afferent or efferent activity of cells in an open-field arrangement (e.g., the pyramidal cells of the cortex that are arranged parallel to each other with all apical dendrites on one side and somata on the other) (Eccles, 1951). Some modeling studies have suggested that stellate cells (classic closed-field generators) also contribute to the EEG (Tenke et al., 1993), though the net contribution from a large population of stellate neurons may be much weaker (due to geometrical cancellation) than the values based on a linear summation of individual neurons (Murakami and Okada, 2006). Early studies demonstrated a close correspondence between EEG activity and synaptic potentials (Creutzfeldt et al., 1966a, 1966b; Klee et al., 1965), indicating that the population excitatory and inhibitory postsynaptic potentials of cortical neurons are major components of the EEG signal. Yet the aforementioned studies had also shown the existence of EEG responses that are not directly coupled to stimulation and do not relate to local cellular activity, such as after-discharges in the form of damped oscillations (Creutzfeldt et al., 1966a, 1966b). Such activity was attributed to larger spatial summation of associational subcortical inputs or cortico-cortical interactions that affect local processing. Indeed, different frequency bands of the extracellularly measured local field potential (LFP), a more localized variant of the EEG, were later shown to reflect other types of neural activity unrelated to synaptic events (Buzsaki and Chrobak, 1995; Kandel and Buzsaki, 1997; Kocsis et al., 1999), including voltage-dependent membrane oscillations and spike afterpotentials. The properties and functional significance of different frequency bands of the LFP signal have recently received increased attention in neuroscience. Studies have reported that LFP bands with higher frequencies are spatially well localized (Goense and Logothetis, 2008), ranging from several hundred micrometers to a few millimeters (Berens et al., 2008; Engel et al., 1990), can clearly differentiate responses that are stimulus related from those that are stimulus unrelated (Belitski et al., 2008; Montemurro et al., 2008) and, most importantly, certain frequency bands can be reliably used to infer spiking activity from nearby neurons during complex naturalistic visual stimulation (Rasch et al., 2008). A question of paramount practical importance is whether different aspects of the EEG signal itself could also provide information regarding the spiking activity of cortical projections neurons, i.e., the output of cortical site.

EEG certainly reflects a much larger integration area than LFPs, and therefore its ability to infer local neural activity (especially spiking activity) must be experimentally verified rather than inferred as an extrapolation from the LFP studies. Moreover, it is particularly important to investigate this in alert monkeys (thereby removing any potential effects of anesthesia, which is known to directly alter the EEG signal), and by using complex natural stimulus conditions (because artificial stimuli might not

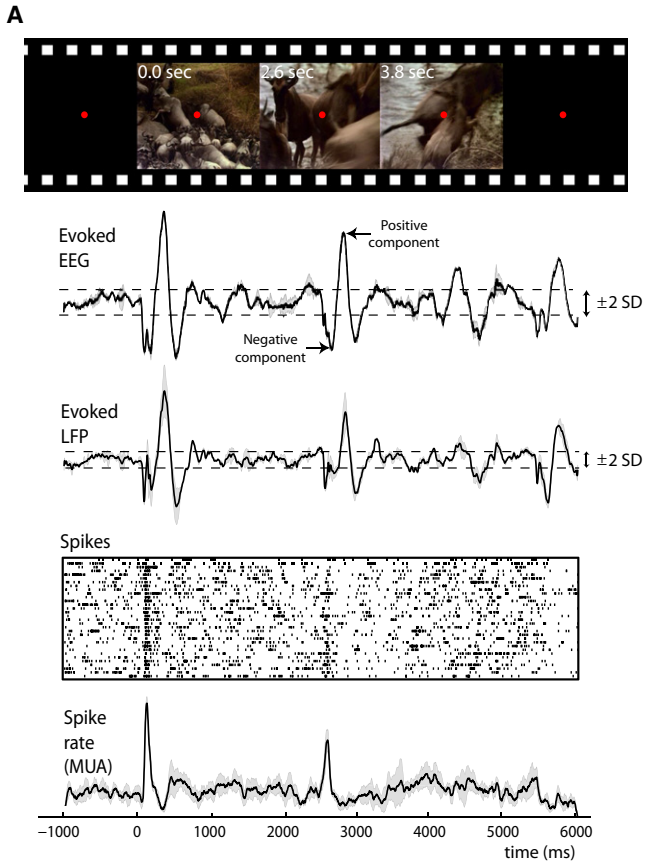

Figure 1. Illustration of Experimental Paradigm and Evoked EEG and LFP Responses, Spike Rasterplot, and Spike Rate (MUA) from a Natural Movie

(A) A small fixation dot on black background was shown in order to indicate the beginning of a trial. After 2 s of fixation, a 5 s movie clip (full field) was presented, followed by 2 s of continued fixation. In this example, three frames from one of the natural movies are shown (white numbers in the top left corner of each movie frame indicate the time at which that particular frame appeared during the movie). Time periods where the evoked EEG and LFP response exceed ± 2 SD of their respective baselines (indicated by the dashed lines) are identified as positive or negative components.

(B) On average (four different movie clips, two monkeys), we found that the MUA associated with negative EEG components is greater than the MUA associated with positive EEG components. Furthermore, the MUA tended to increase relative to its mean (indicated by dashed line labeled "Mean MUA") during negative components, while it decreased during positive components. Error bars represent the standard error of the mean (SEM).

directly generalize to the processing of every day visual input) (Kayser et al., 2004). Therefore, the aim of this study was to determine the features of the EEG signal that yield reliable estimates of different types of neuronal activity, with emphasis on the EEG's ability to predict neuronal spiking of a population of neurons.

To address this question, we simultaneously recorded the surface EEG together with LFP and multiunit activity (MUA) in behaving non-human primates while presenting natural movies. We first characterized the relationship between the well-known visual evoked potential (VEP) and the MUA. We then examined the relationship of power and phase of each frequency band of the EEG signal with MUA.

Overall, we observed that the combination of EEG power in the gamma band (>30 Hz) along with the phase in the delta (2–4 Hz) yielded the most reliable estimate of population spiking activity during attentive visual processing. Specifically, the MUA response was strongest during periods where a burst of gamma power coincided with the negative trough of the ongoing delta wave. In contrast, the MUA response was smaller if a similar burst in gamma power occurred at an arbitrary delta phase.

RESULTS

Evoked Negative EEG Components Coincide with Increased Spiking Activity

Intracortical recordings in the primary visual cortex, in combination with surface EEG were made in two awake, behaving monkeys. Figure 1A shows the trial average of evoked EEG, LFP, and MUA responses from a representative session. The evoked EEG and LFP were positively correlated to each other ($r = 0.25 \pm 0.03$, $p << 0.01$), while we also observed negative correlations for both evoked EEG ($r = -0.12 \pm 0.04$, $p = 0.06$) and LFP ($r = -0.21 \pm 0.03$, $p << 0.01$) with respect to the mean spiking activity (MUA). The evoked EEG response consisted of a series of positive and negative-going deflections that varied in amplitude and latency depending on the movie. We were interested in how such deflections were related to the simultaneously acquired MUA. Therefore, we analyzed time periods where the evoked EEG response exceeded ± 2 standard deviations (SD) of the baseline activity. Within these time periods (which we define as "components"), we calculated the mean MUA activity during positive-going components and negative-going components. On average (two monkeys, four different movies), we found that the MUA associated with negative EEG components tended to be greater than the MUA associated with positive EEG components ($p = 0.0508$, Figure 1B). Additionally, the MUA underlying these negative EEG components was stronger than its mean value over the entire movie time course (dashed line in Figure 1B). In other words, the MUA tended to increase during periods of the movie eliciting a negative EEG component ($p = 0.17$), while the MUA tended to decrease during positive EEG components ($p = 0.16$).

Modulation of Spiking Activity Is Coupled to Low and High, but Not to Midrange, Frequency Power in the EEG

A comparison between power modulations of different EEG bands and the MUA from one representative session is shown

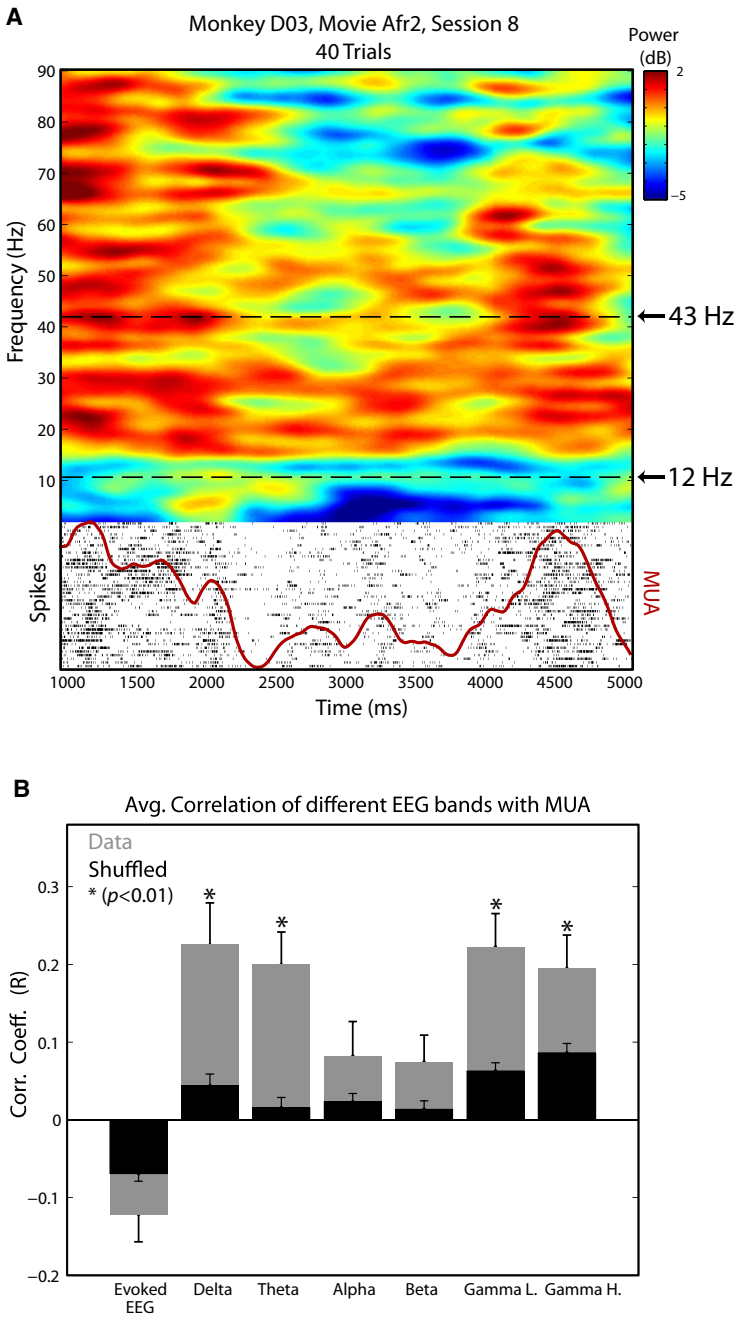

Figure 2. EEG Gamma Power Is Strongly Correlated to Spiking Activity

(A) Time-frequency decomposition of EEG data and corresponding MUA from one experimental session. Modulations in gamma power (e.g., 43 Hz) are closely coupled to MUA, whereas modulations in alpha (e.g., 12 Hz) are not.

(B) Mean correlation coefficient between EEG power modulations in different oscillatory bands with MUA. Error bars represent SEM.

in Figure 2A. In this example, power modulations of gamma activity (for example, at 43 Hz) are closely associated with modulations in MUA. In contrast, modulations in the alpha range (for example, at 12 Hz) are only minimal, and poorly correlated to the MUA. The mean correlation coefficient between modulations in EEG oscillatory power (obtained by band-pass filtering the data into the traditional frequency bands) and MUA, averaged over all experiments in both animals, is shown in Figure 2B. Both low frequency (delta and theta) and high frequency (low gamma and high gamma) power modulations were positively correlated to MUA, whereas midrange oscillations (alpha and beta) were not significantly correlated to MUA (summary of statistics are shown in Table S1 [available online]). Given that these frequency bands are based on human studies that might not be applicable to primates, we additionally performed time-dependent spectral analysis from which we correlated the power of each oscillatory time course (frequency resolution ~1Hz) with the MUA. Here, we found that EEG power modulations in the 11–20 Hz range were not significantly correlated to MUA. This finding was similar to the LFP, where the 9–23 Hz range was not significantly correlated to the MUA (Figure S1). This range of frequencies overlaps the alpha and beta range and is similar to the results we obtained with standard band separation techniques using band-pass filters. Therefore, all subsequent findings reported here are based on band-limited EEG oscillations in the six aforementioned frequency bands.

The observed low correlation between midrange oscillatory power and MUA might reflect slight temporal discrepancies between the two time courses. To rule out temporal offsets as the cause of the low correlation observed between alpha/beta oscillatory power and MUA, we shifted their EEG time courses in various time steps and recalculated their correlation coefficient with MUA. These results are shown in Figure S2. The gamma power showed the strongest correlation with MUA at approximately zero lag, whereas for alpha and beta power the correlation was similar across all time lags, further indicating that modulations in EEG alpha/beta power are indeed uncorrelated to MUA activity.

Correlation between EEG Phase and MUA

To test whether the modulation of phase of different EEG bands carries any information about spiking activity, we extracted the instantaneous phase of each of the six frequency bands and compared it with the corresponding MUA. We computed the probability of finding enhanced MUA (exceeding 5 SD above its baseline) as a function of oscillatory phase. These results are shown in Figure 3A. Rayleigh testing revealed a significant preferred phase-of-firing distribution for delta oscillations (median $p << 0.001$, Figure 3B). That is, enhanced spiking was strongly tuned to the phase of the EEG delta oscillation. In agreement with other studies, we also found that EEG gamma power was significantly tuned to low-frequency phase (data not shown) (Canolty et al., 2006; Lakatos et al., 2005). However, this effect was much weaker than that

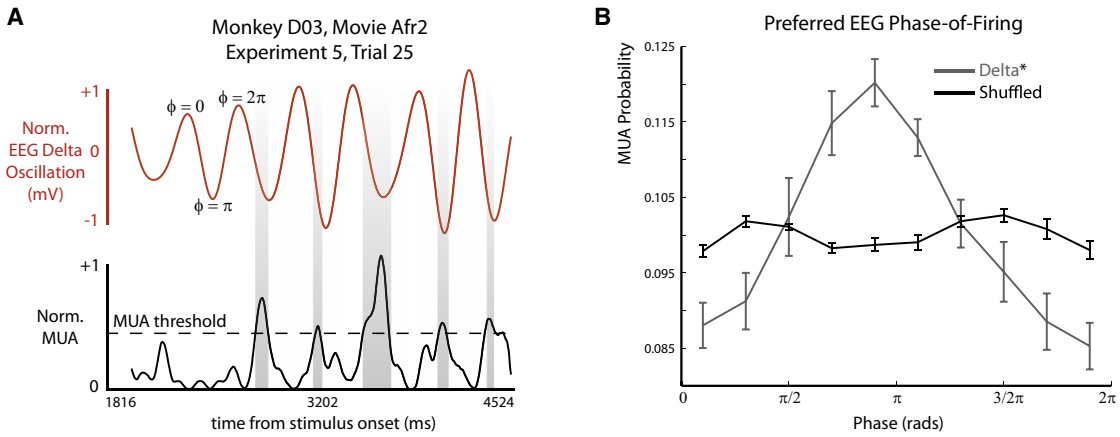

Figure 3. Delta Phase Accompanies Enhanced Spiking Activity

(A) EEG delta oscillation (red trace) and corresponding MUA (black trace) from a single trial. Shaded areas indicate periods where the MUA exceeds 5 SD of its baseline. These specific periods coincided with the negative trough of the delta phase.

(B) MUA strength is significantly tuned to the phase of the delta oscillation (phase-of-firing curve averaged over all data sets). Over all data sets, the mean probability of MUA exceeding 5 SD of its baseline is greatest when the delta oscillation reaches the 0.9π phase value. Error bars represent the standard error of the mean. Shuffled data showed no significant tuning to MUA activity (*$p < 0.001$, Rayleigh test of uniformity).

observed in the MUA (the mean p value obtained from Rayleigh testing was 0.0047 ± 0.0035 for MUA/delta phase and 0.06 ± 0.04 for gamma/delta phase). That is, the coupling between MUA and EEG delta phase was significantly stronger than that observed between EEG gamma power and delta phase. In over 80% of all experimental sessions (acquired from both monkeys), the preferred phase of spiking was in the $[\pi/2, \pi]$ range. This range corresponds to the negative-trough of the delta oscillation, and thus is consistent with our earlier finding where negative evoked components coincided with a high firing rate (Figure 1). It should be noted that theta also had a significant phase-of-firing (Rayleigh test, median p value < 0.01), though was considerably less tuned to the MUA than the delta. The remaining oscillatory bands were not significantly tuned to MUA (Figure S3). Our current EEG observations are directly compatible with earlier findings from our lab (Montemurro et al., 2008) showing robust LFP phase-of firing in anesthetized animals for frequencies below 12 Hz. However, the current analysis suggests that it might be mainly the delta band that shows a particular EEG phase-of-firing in awake, behaving monkeys.

Modeling Spiking Activity from EEG

Given our results, we wanted to know whether the spiking activity from a population of neurons could be modeled by using the surface EEG alone. Put more specifically, we were interested in whether EEG information in the power and phase domain could be combined to estimate the underlying MUA time course. To answer this question, we constructed six general linear models (GLM), each consisting of two regressors. The first regressor consisted of the EEG power time course from one of the six frequency bands; the second, a time course representing the phase of the delta oscillation, normalized to its preferred phase-of-firing. We chose delta as the sole phase regressor given that it had the strongest phase-of-firing probability. An example of GLM construction is shown in Figure 4. The mean goodness-of-fit values (R^2) evaluated for each of the six GLM models are shown in Figure S4A. The distribution of these fits was similar when using LFP data, though the R^2 values were considerably larger (Figure S4B). For EEG data, only models 5 (gamma L. power and delta phase, $p << 0.01$) and 6 (gamma H. power and delta phase, $p << 0.01$) could significantly predict the underlying MUA. F-testing revealed that the phase regressor added significant information to the model which could not be explained by the power alone. Furthermore, their respective beta values were statistically similar ($\beta_{power} = 0.15 \pm 0.03$, $\beta_{phase} = 0.14 \pm 0.02$, $p = 0.70$) indicating that their contribution to modeling the MUA was comparable. Overall, the GLM results reveal two important findings: (1) certain aspects of the EEG signal (e.g., power and phase of individual frequency bands) can be used to reliably estimate modulations in the underlying MUA during presentation of natural movies ($R^2 = 0.12 \pm 0.01$, $p << 0.01$), and (2) the model is not equivalent for all oscillatory bands. There exists only a specific combination of oscillatory power and phase that yields a significant estimate of MUA, whereas the remaining combinations yield low or insignificant MUA fits.

Coupling of Delta Phase and Gamma Power for Inferring Spiking Activity

The GLM results suggest that the MUA is dependent on the specific interaction between high frequency power and low frequency phase (from here on, we refer to this as cross-frequency coupling, or frequency-band coupling). Should this indeed be the case, we would expect to see strong MUA responses when an increase in EEG gamma power coincides with the preferred ($\sim\pi$) delta phase, and weaker MUA responses when similar increases in EEG gamma power appear at a different delta phase. This is highlighted in the two shaded areas of Figure 4 (t_1 and t_2). In Figure 4, increases in gamma power that occur during the preferred delta phase result in increased MUA, which is accurately portrayed by the GLM model (label t_1 in Figure 4E).

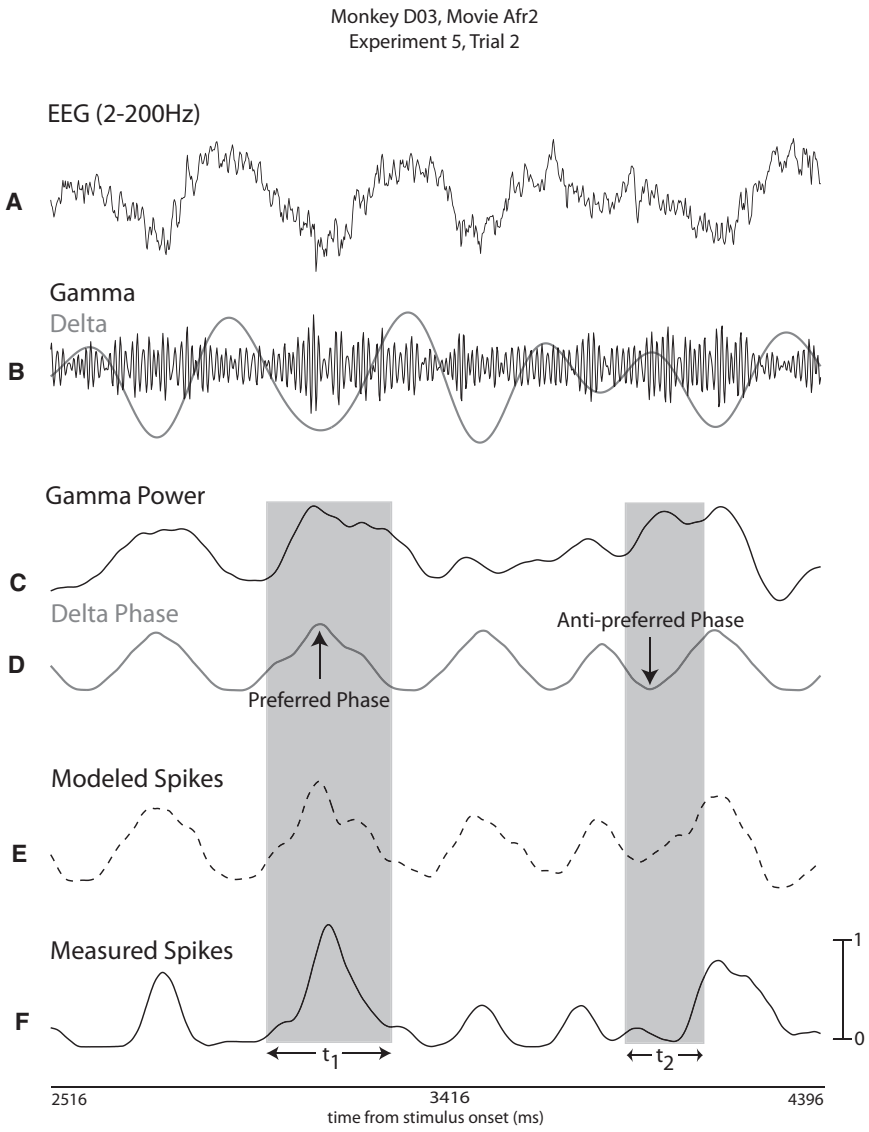

Figure 4. Combined Gamma Power and Delta Phase Can Model Spiking Activity in Single Trials

(A) The broadband surface EEG signal is first filtered into the (B) delta (2–4 Hz) and low gamma (30–60 Hz) band.

(C) Gamma power and (D) delta phase are used as regressors for modeling the MUA (E), which is then compared with the measured MUA (F). Overall, the modeled spiking activity closely resembles the measured spiking activity. For example, in periods where increases in gamma power occur at the preferred delta phase (shaded are t_1), the modeled spiking activity is relatively strong and consistent with the measured spiking activity. In a different time period (shaded are t_2), a similar increase in gamma power coincides with the antipreferred delta phase, yielding a smaller modeled spiking activity that again closely resembles the measured response. In other words, the shaded areas (t_1 and t_2) highlight not only the importance of both gamma power and delta phase for inferring spiking activity, but also how the direct coupling between the two are related to the magnitude of the spiking activity.

DISCUSSION

In the current study, we made simultaneous recordings of surface EEG and spiking activity from a population of neurons in the primary visual cortex (V1) of awake monkeys during the presentation of natural stimuli, i.e., movie clips. To the best of our knowledge, our results unveil for the first time features of the surface EEG signal that correlate best with the concomitant population firing rate (MUA) under natural viewing conditions. Moreover, our examination of the relationship between power and phase of different frequency bands reveals the existence of a coupling mechanism between the power of one band and the phase of another, i.e., FBC. This FBC can be exploited for estimating the relative MUA amplitude solely from the surface EEG.

However, at a different time point (label t_2 in Figure 4E), a similar gamma power is observed as at time point t_1, but it coincides with the antipreferred delta phase. Here, spiking activity is modeled as being low, which is consistent with the measured data. In other words, had only gamma power been used to model the MUA, the GLM would have incorrectly modeled the MUA as having a response equal to that in time point t_1. To investigate this further, we expressed the raw MUA as a function of gamma power and delta phase in single trials and then averaged over all trials and animals. This is shown in Figure 5A. As expected, we found that the MUA increased with increasing gamma power, though delta phase also played a role in shaping the MUA. We found that the MUA was highest only when a high gamma power coincided with the preferred delta phase (Figure 5A). Such robust frequency-band coupling (FBC) was not observed when using shuffled data (Figure 5B) and was weak in other EEG frequency bands (Figure S5). In other words, MUA power depends on the precise interaction between gamma power and delta phase.

We first examined the relationship of MUA with the trial-averaged EEG signal—the so-called VEP that is assumed to reflect synchronous changes of slow postsynaptic potentials occurring within a large number of similarly oriented cortical pyramidal neurons (Nunez, 1981; Schroeder et al., 1991). VEPs usually consist of brief deflections (components) embedded in the background EEG that are commonly characterized by their polarity and latency. They are widely used to study cognitive processes in both basic and clinical research settings, though the cortical events underlying the generation of VEPs under natural stimulus conditions remain poorly understood. We found that the MUA associated with negative-going VEP components was slightly larger compared to positive-going VEP components (Figure 1B). Additionally, the MUA tended to increase (relative to its mean

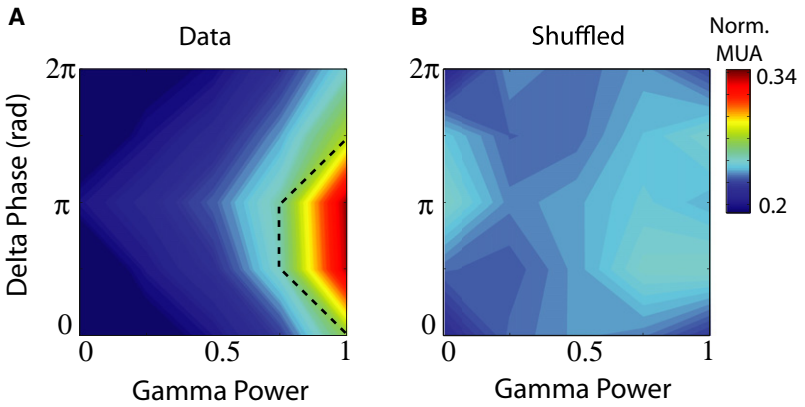

Figure 5. Frequency-Band Coupling of EEG Delta Phase and Gamma Power Is Related to Strength of Spiking Activity

(A) MUA is strongest when increases in gamma power coincide with the preferred delta phase. This is not the case when equally strong gamma coincides with an arbitrary phase, or when using (B) shuffled data. All values to the right of the boundary (dotted line) indicate that MUA values within this region are significantly larger (t test, $p < 0.05$) than the equivalent area in the shuffled data.

activity over the entire movie time course) during negative VEP deflections, which is consistent with previous macaque studies using a combined surface VEP and MUA methodology (Schroeder et al., 1990; Coenen, 1995; Kraut et al., 1985). Our findings that negative VEP components are linked to spiking activity during natural viewing conditions may be used to better interpret VEPs in healthy humans (Whittingstall et al., 2007) and help in noninvasively assessing the effects of different neurological disorders in patients. For instance, in patients with optic neuritis, studies have reported a complete absence of the early negative VEP component though the ensuing positive component is preserved (albeit slightly delayed in time) (Andersson and Siden, 1995).

Although trial-averaged MUA and surface VEP responses are related, it should be noted that the analysis of trial-averaged VEP assumes that evoked components are consistent across trials, which is not always valid (Jung et al., 2001). Therefore, an important test is to further investigate EEG-MUA correlations in single trials. For this, we performed a spectral analysis of the EEG signal and investigated the relationship between EEG oscillations and MUA in single trials. First, we observed significant modulation in the oscillatory power of the EEG and LFP, as well as in the neuronal firing rate while the monkeys were fixating and viewing movies. Our results show that the EEG power in the low and high gamma frequency range (30–100 Hz) is strongly correlated to MUA (Figures 2 and S1). Similar results were found in the LFP signal, which is consistent with other findings linking gamma power and spiking activity in monkey V1 (Belitski et al., 2008; Rasch et al., 2008), rat hippocampus (Csicsvari et al., 2003), and human auditory cortex (Nir et al., 2007). However, alpha (8–15 Hz) and beta (15–30 Hz) power were not correlated to MUA. This finding agrees with, and extends previous work on, LFPs recorded from the anaesthetized macaque (Belitski et al., 2008), and is compatible with the hypothesis that this frequency range is primarily driven by a neuromodulatory pathway not influenced by either the stimulus or the cortical spiking activity (Belitski et al., 2008; Mazzoni et al., 2008). Having shown the relationship between EEG oscillatory power and MUA, we also investigated how the MUA response was modulated at different phases of the EEG. We found that both the firing rate and probability of enhanced firing were greatest during the negative-trough ($\sim\pi$ phase) of the delta (2–4 Hz) oscillation, which is consistent with a recent LFP/MUA study in visual (Lakatos et al., 2008) and auditory cortex (Lakatos et al., 2005). This so-called preferred phase is equivalent to the "ideal" and "high excitability" phase described in earlier studies (Schroeder and Lakatos, 2009). This modulation of firing by the phase was less prominent in the theta (4–8 Hz) and relatively absent in the alpha (8–15 Hz), beta (15–30 Hz) and gamma (>30 Hz) ranges. This finding is well in line with those obtained in auditory cortex (Lakatos et al., 2005, 2008) with the exception that there was also a small coupling of firing to gamma phase in these studies. One methodological explanation for our finding of low coupling between spiking and gamma phase might be that spike-locking to phases of higher frequencies is difficult to detect given that even a small amount of jitter in spike-time precision might abolish locking (in contrast, this effect would be minimal for low frequencies). Such jitter might be introduced during binning of the spike times to our EEG sampling resolution (2 ms). Alternatively, another possibility for a lack of preferred phase of firing for higher-frequency oscillations is that the neurons contributing to the measured spiking activity might lock to different cycles of such high frequencies, as has been suggested for excitatory and inhibitory neurons (Hasenstaub et al., 2005). Compared with shuffled data, we found that the phase-of-firing curves for even the slowest oscillations (delta) were reduced to uniformity, indicating that our observed low-frequency phase of firing is not due to a methodological artifact. Therefore, our findings show that during visual processing, modulations in the firing rate of neurons in the primary visual cortex are closely associated with power in the fast EEG oscillations (>30 Hz) and are locked to the phase of slower oscillations (<8 Hz). In particular, we observed that the MUA amplitude was highest when increases in gamma power occurred during the $\sim\pi$ phase of the delta oscillation (Figure 5A). If similar increases in gamma power coincided with any other delta phase, the observed MUA was reduced, suggesting that the strength of the MUA depends on the interaction between high-frequency power and low-frequency phase (i.e., frequency-band coupling). In other words, we suggest that episodes of EEG coupling between low-frequency phase and high-frequency power serve as a mechanism for inferring spiking activity.

Coupling between frequency bands (so-called cross-frequency coupling) have previously been shown in rodent hippocampus and entorhinal cortex (Csicsvari et al., 2003; Buzsaki et al., 2003; Chrobak and Buzsaki, 1998). Similar results

have since been reported in primate (Lakatos et al., 2005, 2008) and human (Canolty et al., 2006) neocortex. Although our observations are well in line with these, we also reveal that the strength of such coupling can vary substantially over time. We found that the degree of this FBC is directly related to the spiking activity of cortical neurons. This raises important questions regarding the role of such FBC and whether it can facilitate processing of sensory input. In terms of sensory processing, FBC might reflect a mechanism for distinguishing different kinds of information encoded by overlapping neural networks or for organizing the information conveyed with different timescales (Lisman, 2005). For example, bursts of gamma might reflect the activity of cortical networks consisting of mutual inhibitory interactions (Hasenstaub et al., 2005; Wang and Buzsaki, 1996; Bartos et al., 2007; Whittington et al., 1995) or interactions between excitatory and inhibitory neurons (Jefferys et al., 1996; Mann et al., 2005). Delta-band oscillations, however—long believed to reflect periods of deep sleep (Steriade, 2006)—have recently been shown to be both stimulus informative (Montemurro et al., 2008) and linked to attentional selection (Lakatos et al., 2008). We observed, in both stimulus and stimulus-free periods, that the spiking activity was highest during the delta trough (Figure S6). That is, the observed coupling between delta phase and MUA cannot be entirely explained by the visual stimulus. Therefore, delta oscillations in V1 might also, at least in part, reflect internally generated cyclical variations in the excitability of a neuronal ensemble and thus contain important information regarding the state of the network. That is, inputs that arrive during the high-excitability delta phase are amplified, whereas those arriving during the low-excitability phase are suppressed (Schroeder et al., 2008). Therefore, FBC might provide a mechanism whereby a weak, subthreshold input becomes effective in discharging a population of neurons that might play a role in efficiently encoding the stimulus. This is supported by a recent MEG study in humans showing that periods of strong cross-frequency coupling (i.e., amplitude modulations in the gamma range that are locked to the phase of the delta band) accurately reflect success in a visual discrimination task (Handel and Haarmeier, 2009). However, our observation of (albeit weak) FBC during stimulus-free periods suggests that the relationship between EEG and spiking activity is not solely shaped by the visual stimulus alone and might reflect a more general phenomenon of cortical processing. This is in agreement with earlier studies that found that the structure of spontaneous neural activity can resemble stimulus-driven activity (Fiser et al., 2004; Kenet et al., 2003). Although a complete description of the neural events underlying FBC is beyond the scope of this study, our findings nevertheless show how this relatively simplistic model serves as a basis for linking surface EEG activity to the spiking activity from a population of cortical neurons. This information can now be used to better interpret noninvasively obtained EEG signals with respect to their underlying neural events.

EXPERIMENTAL PROCEDURES

Data Acquisition

Electrophysiological data recorded from two nonanesthetized monkeys (*Macaca mulatta*) are included in the present study. All animal experiments were approved by the local authorities (Regierungspräsidium Tübingen) and are in full compliance with the guidelines of the European Community (EUVD 86/609/EEC) for the care and use of laboratory animals. EEG recordings were made using an Ag/AgCl ring electrode positioned over the visual cortex. Electrode impedance was kept below 20 kΩ. EEG signals were amplified and filtered into a band of 0.2–250 Hz (Brain Products, Munich, Germany) and digitized at 5 kHz. The EEG ring electrode of interest was placed at the base of a recording chamber made from PEEK (polyetheretherketone; TecaPEEK, Nufringen, Germany), which was secured to the skull with custom-made ceramic screws. The EEG ring electrode rested on the skull and small circular openings (under the center of the EEG ring electrode) in the skull were made to access cortical neurons. In one monkey (D02), a 5 mm circular patch was resected, while in monkey A03, a 2 mm circular patch (~2 mm diameter) was resected in order to access the underlying cortex. Surgical procedures are described elsewhere together with hardware details of the recording setup (Logothetis et al., 2002). Tungsten microelectrodes (FHC, Bowdoinham, ME) were lowered through the middle of the EEG ring electrode into the cortex. Electrode tips were typically (but not always) positioned in the upper or middle cortical layers. The impedance of the electrode varied from 500 kΩ to 2 MΩ. The signals were amplified and filtered into a band of 1–8 kHz (alpha Omega Engineering, Nazareth, Israel) and then digitized at 20.833 kHz with 16-bit resolution (National Instruments, Austin, TX), ensuring enough resolution for both local field and spiking activities. A frontal EEG electrode placed on the scalp was used as reference.

Visual Stimulation

Visual stimuli were delivered via computer screen (refresh rate 90Hz) placed at eye level, 190 cm in front of the monkey. Eye movements were continuously monitored with an infrared camera (RealEye, Avotec, Stuart, FL) with eye-tracking software (iView, Sensomotoric Instruments GmbH, Teltow, Germany). A small fixation point (0.2°) on black background was shown in order to indicate the beginning of the trial. After 2 s of fixation, a 5 s movie segment (full field) was presented, followed by 2 s of continued fixation, resulting in trials totaling 9 s of fixation. In trials where fixation was held throughout, the monkey received a juice reward, whereas trials where the monkey broke fixation were immediately aborted. Movie clips consisted of fast-moving and colorful clips (no soundtrack) from commercially available movies. Behavioral tasks (including movie onset/offset times) were controlled by computers running a real-time OS (QNX, Ottawa, Canada) (Sheinberg and Logothetis, 2001).

Data Analysis

All data analysis procedures were implemented with the Matlab programming language (Mathworks, Natick, MA) in combination with the EEGlab analysis toolbox (Delorme and Makeig, 2004) as described below.

Multiunit Activity Analysis

We used a publicly available spike-sorting algorithm for semiautomatic detection of spike times (Quiroga et al., 2004). Briefly, the algorithm filters the LFP signal between 300 and 3500 Hz, and an amplitude threshold of 4 SD of the mean amplitude is used for spike detection. A spike was recognized as such only if the last spike occurred more than 1.5 ms earlier. This threshold approach for spike detection is appropriate for spike times but not for the isolation of single units. Thus, the spikes used for the analysis represented the spiking activity of a small population of cells rather than well separated spikes from single neurons. Spike rates (also referred to in this study as MUA) were obtained using 10 ms windows.

Data Filtering and Spectral Analysis

EEG and neural (MUA and LFP) signals were first re-referenced to the frontal electrode site, and then downsampled to 500 Hz. For all subsequent analysis, we discarded the first second of data because it mainly consisted of a transient response to the stimulus onset. Evoked signals were obtained by averaging the broadband signals (2–200 Hz) across trials. Evoked components were identified as periods of the movie where the signal amplitude exceeded 2 SD of the baseline. For oscillatory analysis, EEG and LFP data were band-passed filtered into the traditional EEG bands: delta (2–4 Hz), theta (4–8 Hz), alpha (8–15 Hz), beta (15–30 Hz), low (30–60 Hz), and high (60–100 Hz) gamma

using a bidirectional FIR filter, which eliminates the effects of possible phase shifts introduced by the filtering process. In each trial, we computed the envelope of each band-limited oscillation by calculating the magnitude of its Hilbert transform, averaged it across trials, and then calculated the correlation coefficient (R) between it and the trial-averaged MUA. For comparison purposes, time-frequency analysis was carried out by computing a spectrogram in each trial using overlapping 512 ms windows that were stepped at an average value of 32 ms, and then averaged over all trials. We calculated the correlation coefficient between each oscillatory time course in the spectrogram (0.97 Hz resolution, 0.98–199.2 Hz) with the trial-averaged MUA (MUA time courses were resampled to match the temporal resolution of the spectrogram). For phase analysis, we calculated the angle of the Hilbert transform and extracted the instantaneous phase [0,2π] in each of the six band-limited oscillations in single trials. Phase-of-firing curves were calculated by extracting MUA values that were greater than 5 SD of the baseline along with their corresponding EEG phase value. FBC diagrams were constructed in single trials as follows: the band-limited phase ([0, 2π]) and normalized power ([0, 1]) were each divided into 5 equally spaced segments (totaling 25 possible segment combinations). We then extracted the MUA that fell within the aforementioned segments (for example, the first range would consist of all MUA values corresponding to EEG phase values ranging from [0, .4π] and normalized EEG power ranging from [0, 0.1]) and computed the mean.

General Linear Modeling

We used general linear modeling to investigate whether information in the EEG signal can be used to model the underlying MUA. In particular, we were interested in which of the six band-limited EEG oscillatory bands was the best predictor of MUA. The GLM model consisted of three regressors: (1) EEG oscillatory power, (2) EEG oscillatory phase, and (3) a constant term, which is expressed as:

$$Y = \beta_1 X_1 + \beta_2 X_2 + \varepsilon$$

where Y is the measured MUA, $X_{1,2}$ is the oscillatory power and phase (respectively), $\beta_{1,2}$ are the weights of the power and phase, and ε is the error term. GLM analysis was carried out in each single trial of each experiment. The MUA and oscillatory power were normalized to their peak value in each single trial. The phase regressor was created by normalizing the instantaneous phase to its peak phase-of-firing probability in each single trial. Therefore, the phase regressor (β_2) consisted of a time course (equal in length to Y and β_1) that varied from its "preferred phase" to its "anti-preferred phase." The single trial GLM results were then averaged across experiments and animals.

Testing for Statistical Significance

On any given experimental session, we recorded neural activity using two or three different movie clips as stimulus. In order to test for statistical significance, we compared all results obtained with the methods described above to the results obtained when using mismatched data sets. For example, in the correlation analysis, we randomly selected MUA obtained in one movie and correlated it with the EEG from a different movie clip. This procedure was repeated a total of 200 times in order to obtain a reliable estimate of the desired calculation. These "shuffled" results were then compared with the "true" results using a paired t test.

SUPPLEMENTAL DATA

Supplemental Data include six figures and one table can be found with this article online at http://www.neuron.org/supplemental/S0896-6273(09)00628-X.

ACKNOWLEDGMENTS

We would like to thank Stefano Panzeri and Andreas Bartels for helpful discussions on data analysis and statistics; Yusuke Murayama, Joachim Werner, and Axel Oeltermann for help in the acquisition of data; Stefan Weber for fine-mechanic work, and Ulrich Schridde, Matthias Munk, and Jozien Goense for comments on an earlier version of the manuscript. This research was supported by the Max Planck Society.

Accepted: August 21, 2009
Published: October 28, 2009

REFERENCES

Andersson, T., and Siden, A. (1995). An analysis of VEP components in optic neuritis. Electromyogr. Clin. Neurophysiol. *35*, 77–85.

Bartos, M., Vida, I., and Jonas, P. (2007). Synaptic mechanisms of synchronized gamma oscillations in inhibitory interneuron networks. Nat. Rev. Neurosci. *8*, 45–56.

Belitski, A., Gretton, A., Magri, C., Murayama, Y., Montemurro, M.A., Logothetis, N.K., and Panzeri, S. (2008). Low-frequency local field potentials and spikes in primary visual cortex convey independent visual information. J. Neurosci. *28*, 5696–5709.

Berens, P., Keliris, G.A., Ecker, A.S., Logothetis, N.K., and Tolias, A.S. (2008). Comparing the feature selectivity of the gamma-band of the local field potential and the underlying spiking activity in primate visual cortex. Front. Syst. Neurosci. *2*, 2.

Buzsaki, G., and Chrobak, J.J. (1995). Temporal structure in spatially organized neuronal ensembles: a role for interneuronal networks. Curr. Opin. Neurobiol. *5*, 504–510.

Buzsaki, G., Buhl, D.L., Harris, K.D., Csicsvari, J., Czeh, B., and Morozov, A. (2003). Hippocampal network patterns of activity in the mouse. Neuroscience *116*, 201–211.

Canolty, R.T., Edwards, E., Dalal, S.S., Soltani, M., Nagarajan, S.S., Kirsch, H.E., Berger, M.S., Barbaro, N.M., and Knight, R.T. (2006). High gamma power is phase-locked to theta oscillations in human neocortex. Science *313*, 1626–1628.

Chrobak, J.J., and Buzsaki, G. (1998). Gamma oscillations in the entorhinal cortex of the freely behaving rat. J. Neurosci. *18*, 388–398.

Coenen, A.M. (1995). Neuronal activities underlying the electroencephalogram and evoked potentials of sleeping and waking: implications for information processing. Neurosci. Biobehav. Rev. *19*, 447–463.

Creutzfeldt, O.D., Watanabe, S., and Lux, H.D. (1966a). Relations between EEG phenomena and potentials of single cortical cells. I. Evoked responses after thalamic and erpicortical stimulation. Electroencephalogr. Clin. Neurophysiol. *20*, 1–18.

Creutzfeldt, O.D., Watanabe, S., and Lux, H.D. (1966b). Relations between EEG phenomena and potentials of single cortical cells. II. Spontaneous and convulsoid activity. Electroencephalogr. Clin. Neurophysiol. *20*, 19–37.

Csicsvari, J., Jamieson, B., Wise, K.D., and Buzsaki, G. (2003). Mechanisms of gamma oscillations in the hippocampus of the behaving rat. Neuron *37*, 311–322.

Delorme, A., and Makeig, S. (2004). EEGLAB: an open source toolbox for analysis of single-trial EEG dynamics including independent component analysis. J. Neurosci. Methods *134*, 9–21.

Eccles, J.C. (1951). Interpretation of action potentials evoked in the cerebral cortex. Electroencephalogr. Clin. Neurophysiol. *3*, 449–464.

Engel, A.K., Konig, P., Gray, C.M., and Singer, W. (1990). Stimulus-dependent neuronal oscillations in cat visual cortex: inter-columnar interaction as determined by cross-correlation analysis. Eur. J. Neurosci. *2*, 588–606.

Fiser, J., Chiu, C., and Weliky, M. (2004). Small modulation of ongoing cortical dynamics by sensory input during natural vision. Nature *431*, 573–578.

Goense, J.B., and Logothetis, N.K. (2008). Neurophysiology of the BOLD fMRI signal in awake monkeys. Curr. Biol. *18*, 631–640.

Handel, B., and Haarmeier, T. (2009). Cross-frequency coupling of brain oscillations indicates the success in visual motion discrimination. Neuroimage *45*, 1040–1046.

Hasenstaub, A., Shu, Y., Haider, B., Kraushaar, U., Duque, A., and McCormick, D.A. (2005). Inhibitory postsynaptic potentials carry synchronized frequency information in active cortical networks. Neuron *47*, 423–435.

Jefferys, J.G., Traub, R.D., and Whittington, M.A. (1996). Neuronal networks for induced '40 Hz' rhythms. Trends Neurosci. *19*, 202–208.

Jung, T.P., Makeig, S., Westerfield, M., Townsend, J., Courchesne, E., and Sejnowski, T.J. (2001). Analysis and visualization of single-trial event-related potentials. Hum. Brain Mapp. *14*, 166–185.

Kandel, A., and Buzsaki, G. (1997). Cellular-synaptic generation of sleep spindles, spike-and-wave discharges, and evoked thalamocortical responses in the neocortex of the rat. J. Neurosci. *17*, 6783–6797.

Kayser, C., Kording, K.P., and Konig, P. (2004). Processing of complex stimuli and natural scenes in the visual cortex. Curr. Opin. Neurobiol. *14*, 468–473.

Kenet, T., Bibitchkov, D., Tsodyks, M., Grinvald, A., and Arieli, A. (2003). Spontaneously emerging cortical representations of visual attributes. Nature *425*, 954–956.

Klee, M.R., Offenloch, K., and Tigges, J. (1965). Cross-correlation analysis of electroencephalographic potentials and slow membrane transients. Science *147*, 519–521.

Kocsis, B., Bragin, A., and Buzsaki, G. (1999). Interdependence of multiple theta generators in the hippocampus: a partial coherence analysis. J. Neurosci. *19*, 6200–6212.

Kraut, M.A., Arezzo, J.C., and Vaughan, H.G., Jr. (1985). Intracortical generators of the flash VEP in monkeys. Electroencephalogr. Clin. Neurophysiol. *62*, 300–312.

Lakatos, P., Karmos, G., Mehta, A.D., Ulbert, I., and Schroeder, C.E. (2005). An oscillatory hierarchy controlling neuronal excitability and stimulus processing in the auditory cortex. J. Neurophysiol. *94*, 1904–1911.

Lakatos, P., Shah, A.S., Knuth, K.H., Ulbert, I., Karmos, G., and Schroeder, C.E. (2008). Entrainment of neuronal oscillations as a mechanism of attentional selection. Science *320*, 110–113.

Lisman, J. (2005). The theta/gamma discrete phase code occuring during the hippocampal phase precession may be a more general brain coding scheme. Hippocampus *15*, 913–922.

Logothetis, N., Merkle, H., Augath, M., Trinath, T., and Ugurbil, K. (2002). Ultra high-resolution fMRI in monkeys with implanted RF coils. Neuron *35*, 227–242.

Lopes da Silva, F., and Van Rotterdam, A. (1987). Biophysical aspects of EEG and MEG generation. In Electroencephalography: Basic Principles, Clinical Applications and Related Fields, E. Neidermeyer and F.H. Lopes da Silva, eds. (Baltimore: Urban & Schwarzenberg), pp. 15–28.

Mann, E.O., Radcliffe, C.A., and Paulsen, O. (2005). Hippocampal gamma-frequency oscillations: from interneurones to pyramidal cells, and back. J. Physiol. *562*, 55–63.

Mazzoni, A., Panzeri, S., Logothetis, N.K., and Brunel, N. (2008). Encoding of naturalistic stimuli by local field potential spectra in networks of excitatory and inhibitory neurons. PLoS Comput. Biol. *4*, e1000239.

Montemurro, M.A., Rasch, M.J., Murayama, Y., Logothetis, N.K., and Panzeri, S. (2008). Phase-of-firing coding of natural visual stimuli in primary visual cortex. Curr. Biol. *18*, 375–380.

Murakami, S., and Okada, Y. (2006). Contributions of principal neocortical neurons to magnetoencephalography and electroencephalography signals. J. Physiol. *575*, 925–936.

Nir, Y., Fisch, L., Mukamel, R., Gelbard-Sagiv, H., Arieli, A., Fried, I., and Malach, R. (2007). Coupling between neuronal firing rate, gamma LFP, and BOLD fMRI is related to interneuronal correlations. Curr. Biol. *17*, 1275–1285.

Nunez, P.L. (1981). Electric Fields of the Brain: The Neurophysics of EEG (Oxford, UK: Oxford University Press).

Quiroga, R.Q., Nadasdy, Z., and Ben-Shaul, Y. (2004). Unsupervised spike detection and sorting with wavelets and superparamagnetic clustering. Neural Comput. *16*, 1661–1687.

Rasch, M.J., Gretton, A., Murayama, Y., Maass, W., and Logothetis, N.K. (2008). Inferring spike trains from local field potentials. J. Neurophysiol. *99*, 1461–1476.

Schroeder, C.E., and Lakatos, P. (2009). Low-frequency neuronal oscillations as instruments of sensory selection. Trends Neurosci. *32*, 9–18.

Schroeder, C.E., Tenke, C.E., Givre, S.J., Arezzo, J.C., and Vaughan, H.G., Jr. (1991). Striate cortical contribution to the surface-recorded pattern-reversal VEP in the alert monkey. Vision Res. *31*, 1143–1157.

Schroeder, C.E., Tenke, C.E., Givre, S.J., Arezzo, J.C., and Vaughan, H.G., Jr. (1990). Laminar analysis of bicuculline-induced epileptiform activity in area 17 of the awake macaque. Brain Res. *515*, 326–330.

Schroeder, C.E., Lakatos, P., Kajikawa, Y., Partan, S., and Puce, A. (2008). Neuronal oscillations and visual amplification of speech. Trends Cogn. Sci. *12*, 106–113.

Sheinberg, D.L., and Logothetis, N.K. (2001). Noticing familiar objects in real world scenes: the role of temporal cortical neurons in natural vision. J. Neurosci. *21*, 1340–1350.

Steriade, M. (2006). Grouping of brain rhythms in corticothalamic systems. Neuroscience *137*, 1087–1106.

Tenke, C.E., Schroeder, C.E., Arezzo, J.C., and Vaughan, H.G., Jr. (1993). Interpretation of high-resolution current source density profiles: a simulation of sublaminar contributions to the visual evoked potential. Exp. Brain Res. *94*, 183–192.

Wang, X.J., and Buzsaki, G. (1996). Gamma oscillation by synaptic inhibition in a hippocampal interneuronal network model. J. Neurosci. *16*, 6402–6413.

Whittingstall, K., Stroink, G., and Schmidt, M. (2007). Evaluating the spatial relationship of event-related potential and functional MRI sources in the primary visual cortex. Hum. Brain Mapp. *28*, 134–142.

Whittington, M.A., Traub, R.D., and Jefferys, J.G. (1995). Synchronized oscillations in interneuron networks driven by metabotropic glutamate receptor activation. Nature *373*, 612–615.